Journal of Cleaner Production 415 (2023) 137785

Contents lists available at ScienceDirect

Journal of Cleaner Production

journal homepage: www.elsevier.com/locate/jclepro

Optimizing desalination for regional water systems: Integrating uncertainty, quality, and sustainability

Greg Hendrickson [a], Mashor Housh [b], Lina Sela [a,*]

[a] The University of Texas at Austin, Austin, TX, 78712, United States
[b] University of Haifa, Haifa, 3498838, Israel

ARTICLE INFO

Handling Editor: Kathleen Aviso

Keywords:
Water resources system
Desalination
Mixed water qualities
Uncertainty
Optimal management

ABSTRACT

Regional water supply systems in arid regions worldwide face growing challenges due to increasing demands under conditions of water scarcity. For coastal regions, the addition of seawater desalination as an alternative water source can hedge against uncertainty stemming from demands placed on the system and hydrological inputs to the natural resources. In order to effectively integrate desalination into a water supply system, water managers utilize optimization models that solve for the optimal mix of desalination and natural resources to meet consumer demands at a sufficient water quality while maintaining sustainable levels in the natural resources. The complexity of managing both quantity and quality for a water supply system facing uncertainties is increased by contractual limitations between desalination plant owners and water managers that dictate the desalination production decisions to occur at the start of the year before the uncertainties have been revealed. To incorporate the misalignment between decision timelines and the order in which the uncertainty is revealed, a two-stage optimization approach is utilized where management decisions are split into implementable decisions representing the desalination production volumes, and recourse decisions representing supply volumes from the remaining sources and water allocations in the supply network. An iterative process is then undertaken in which in the first stage the implementable decisions are solved for potential uncertain scenarios, and then introduced to the second stage as inputs where the recourse decisions are iteratively solved for new uncertain scenarios. This framework is applied to the Israeli national water supply system, where the unique challenges of managing mixed salinity sources and asynchronous decision timelines in the face of uncertainty are addressed. A multicriteria decision analysis method is then applied where tradeoffs are found between the upfront investment in desalination and the expected system operational cost and robustness to failure. The inclusion of multicriteria decision analysis to analyze the multiple desalination production alternatives allows for including stakeholders preferences in model-based decision-making.

1. Introduction

Water supply systems (WSS) worldwide have to effectively withstand uncertainty in population growth and future climate conditions in order to overcome water stress. For many such systems, desalination has become a robust alternative water source for its ability to convert non-potable sources such as seawater and brackish water into potable water, while maintaining flows irrespective of drought conditions (Avni et al., 2013). The total volume of water produced from desalination plants globally has increased from 13 million cubic meter per day (MCMD) in 2000 to 95 MCMD in 2019 (Jones et al., 2019). As technological advances drive down the cost of desalination and water scarcity in natural resources increases the cost of conventional water supply, desalination is increasingly becoming a cost-competitive alternative (Sood and Smakhtin, 2014). Furthermore, by 2050 population growth combined with decreasing natural resource availability is expected to double the total volume of water produced by desalination (Darre and Toor, 2018). Regional water systems generally have a variety of consumers (e.g., municipal, industrial, and agricultural) with diverse water quality requirements, where desalination can be combined with other water sources (e.g., aquifers, surface water, and reclaimed water) to meet the specific needs of each consumer (Slater et al., 2020). As global weather patterns are expected to face increased variability leading to more extreme and

* Corresponding author.
E-mail address: linasela@utexas.edu (L. Sela).

https://doi.org/10.1016/j.jclepro.2023.137785
Received 2 February 2023; Received in revised form 7 June 2023; Accepted 10 June 2023
Available online 15 June 2023
0959-6526/

frequent events such as droughts (Dore, 2005), it is imperative that water managers foresee scarcity events in order to leverage drought-resistant desalination supply ahead of time to overcome future deficits in natural resources (Slater et al., 2020).

To determine the operation of regional WSSs, water management models can be used to mathematically define the objectives of water managers and constraints imposed on the system via physical laws and other system requirements (Loucks and Van Beek, 2017). Depending on management goals and system characteristics, water management models can differ in the types of decision variables incorporated and the timelines in which decisions are made. Traditional models applied at the regional scale focus on decisions related to water quantities, solving for both the volume of water to be utilized from each source and how those volumes are distributed in the system to various consumers. Such models have been used in the past to minimize the operational cost of a system while meeting demand requirements from consumers (e.g., Draper et al. (2003), Jenkins et al. (2004) and Watkins et al. (2004)), maximize the total net benefits between competing parties through compromises in water usage (e.g., Fisher et al. (2002) and Booker et al. (2005)), and foster conjunctive use between surface and groundwater sources (Pulido-Velázquez et al., 2006). For systems with diverse source qualities and consumer quality thresholds, WSS management models also include nonlinear solute mass balances where solute concentrations are included as decision variables (Mehrez et al., 1992). Such quantity–quality models have been applied to various regional WSSs to find optimal source production and water allocations at steady-state (e.g., Ostfeld and Shamir (1993), Alidi and Al-Faraj (1994) and Cohen et al. (2000)) over a short-term horizon (Tu et al., 2005), and over a long-term horizon (Housh et al., 2012). In the case of a WSS with supply from desalination plants, salinity is often the water quality parameter of concern, and quantity–quality optimization models can be applied to find the optimal blending of desalinated water with other sources with different salinity levels to meet the water quality thresholds for municipal, agricultural, and industrial consumers (Slater et al., 2020). While providing a low-salinity, drought resistant supply, the introduction of desalination to a regional water supply portfolio introduces challenges for water managers through high energy costs (Shemer and Semiat, 2017; Vahid Pakdel et al., 2020), decreased mineral composition in supply water (Avni et al., 2012, 2013), and brine production requiring disposal (Ahmed et al., 2001; Khan and Al-Ghouti, 2021). An additional challenge for water managers is the decision timeline for desalination plants, where complex contractual agreements require water production to be decided in advance before the future conditions are known (Israeli Ministry of Finance, 2022). Hence, the desalination productions decisions are made ahead of time using forecasted uncertain scenarios, while the remaining decisions, such as supply from the natural resources and water allocations in the system, can be made at a later stage once the uncertainty is revealed. In a management model, the disparate decision timelines can be handled by splitting the decision variables into *here-and-now* decisions and *wait-and-see* decisions, where the former are made against forecasted scenarios, and the latter are made in response to the revealed scenarios (Ben-Tal et al., 2004). Through the inclusion of asynchronous decision timelines for water quantity and quality variables, water managers are able to model the behavior of multi-quality systems under uncertain conditions while reflecting the chronological sequence of decision-making.

Two of the primary sources of uncertainty for water supply systems include consumer demands and hydrological inflows (Cosgrove and Loucks, 2015). In the long-term, demand uncertainty is primarily defined by uncertain population growth and in the short-term, by uncertain consumer behavior and natural variability (Dandy et al., 2023). Uncertainty in hydrological inflows is connected more broadly to hydroclimatic uncertainty, where precipitation, snowmelt runoff, and other climate-influenced hydrological processes affect replenishment of natural water resources (McMillan et al., 2018). Recent trends have indicated a loss of stationarity in historical record, where the likelihood for extreme events such as prolonged droughts are expected to increase in many regions (Parry et al., 2007). The traditional approach to handling uncertainty is to operate under the assumption that the expected scenario will occur, and optimize the decisions in response (Perelman et al., 2013). However, when the revealed uncertainty deviates from the expected scenario, the final model decisions can result in non-optimal or infeasible solutions (Sen and Higle, 1999). Furthermore, for quantity–quality models that are nonlinear in nature, small deviations from the expected values of the uncertain parameters can result in large deviations in the final solution which means that water systems are at risk of going over-budget or not meeting system requirements (Housh, 2011). In this research, uncertainty is characterized by a set of scenarios that represent different possibilities for consumer demands in the system and hydrological inflows to the natural resources. Scenario-based methods have been utilized by decision-makers to solve for a range of water resources management problems, including watershed management (Liu et al., 2007), planning of water and wastewater infrastructure (Kang and Lansey, 2013), and long-term planning for expanding the capacity of water sources (Ray et al., 2012). The use of scenario-based methods is appropriate when details of the probability distributions underlying the uncertain parameters are themselves unknown. When there is insufficient data to build accurate distributions or the distributions are no longer characteristic of the uncertainty, such as with non-stationary processes, methods that incorporate unknown distributions directly into the optimization model can result in sub-optimal solutions (Herman et al., 2014). In contrast, scenario-based approaches find optimal solutions for each individual scenario, thereby producing a set of non-dominant solutions that can be assessed a posteriori based on stakeholder preferences. The result is an effective characterization of uncertainty without relying on a precise probability distribution.

Beyond the technical benefits of the scenario-based approach, the utilization of scenarios is beneficial for stakeholders who are not involved in the modeling process, as solving for individual scenarios and comparing the different solutions is an intuitive method for incorporating uncertainty (Kang and Lansey, 2013). However, the differing solutions may consist of many tradeoffs between stakeholder objectives where no solution is clearly superior. Multicriteria decision analysis (MCDA) is a method to integrate stakeholder preferences into the decision-making process and use them to differentiate between alternative solutions and elucidate inherent tradeoffs (Morais and Almeida, 2007). For a water system, common preferences might include economic considerations such as minimal operating costs, performance considerations such as the satisfaction of consumer demands and fulfillment of water quality standards, or other preferences specific to the system being considered (Haimes, 1977). MCDA methods have been used to explore tradeoffs in water systems to manage water losses (Morais and Almeida, 2006), develop long-term management strategies (Pudenz et al., 2002), improve the operation of a two-reservoir system (Srdjevic et al., 2004), and plan for the feasibility and site-selection of desalination infrastructure (Vishnupriyan et al., 2021). As stated by Gough and Ward (1996), the primary characteristics of environmental decision-making include the existence of considerable uncertainty, the potential for decisions that lead to irreversible outcomes, and the combination of multiple decision-makers and objectives. Given these circumstances for a regional water supply system, a scenario-based optimization model in conjunction with MCDA serves as a tool to aid in the decision-making process by properly assessing the uncertainty and providing interpretable results to the relevant stakeholders.

It follows that the goal of this research is to provide a modeling tool for decision-makers managing regional water supply systems that blends desalination sources with natural resources throughout the water network in order to provide the optimal water quantity and quality to the different consumers. The primary challenges for such

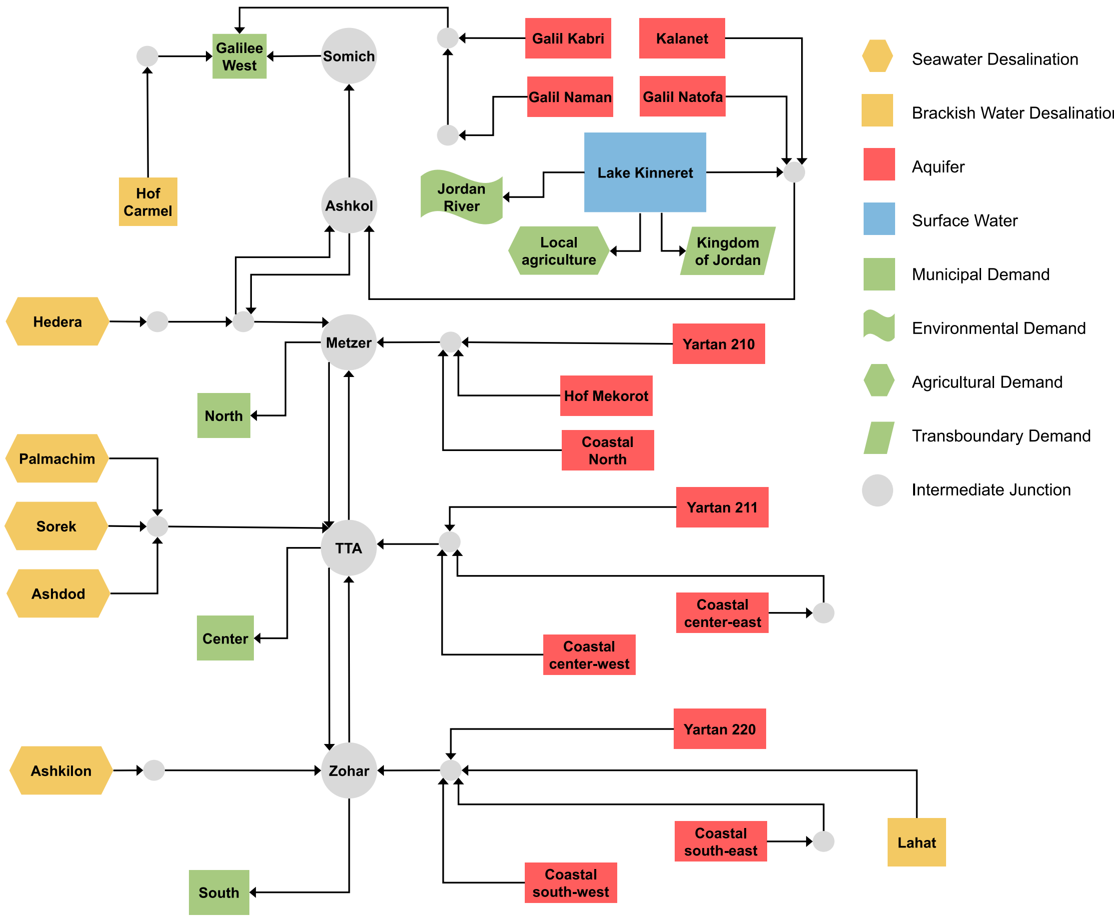

Fig. 1. INWSS schematic.

a system are (1) multi-quality sources and diverse consumers, (2) disparate decision timelines, and (3) uncertainty in consumer demands and hydrological inflows. To address these challenges, an optimization approach is proposed that combines (1) nonlinear constraints for salinity considerations (2) a two-stage approach to handle differing decision timelines, and (3) a scenario-based method that solves the nonlinear optimization model for different potential scenarios in both modeling stages. The final results of the optimization model are analyzed using a MCDA approach to assess tradeoffs in operational cost and system robustness in order to help facilitate decision-making for future desalination production as a potential hedge against uncertain conditions. The result is a unified modeling framework that is applied to the Israeli National Water Supply System (INWSS) where desalination is combined with aquifers and surface water to supply municipal and agricultural demands, as well as transboundary water transfers. Given the increasing incorporation of desalination plants into regional water supply systems worldwide combined with increasing variability in global climate conditions, insights gained from the INWSS can be an important source for other regional system seeking to secure their future water supply.

2. Methodology

In this section we propose a framework to aid decision-makers in the management of a multi-quality regional water supply system, where the system faces uncertainties in hydrological inflows and consumer demands. First, we introduce the study area and problem. Second, we propose a two-stage optimization framework to manage the desalination flow rates, where in Stage I, the desalination decisions are solved against forecasted uncertainty, and in Stage II, the desalination decisions are provided as inputs and the model is tested against new realizations of uncertainty. Third, the results of the two-stage model are distilled into performance metrics that represent the operational cost and system robustness. Finally, a multicriteria decision analysis method is showcased for analyzing the performance tradeoffs found in the decision alternatives and assisting decision-makers in evaluating and choosing between them.

2.1. Problem definition

2.1.1. Israeli national water supply system

The water management framework is applied to the INWSS, which is responsible for delivering water from Israel's supply sources to local water suppliers through a central conveyance system (Housh et al., 2012). Historically, the primary water sources include groundwater aquifers and Lake Kinneret, however, as the demand for water increased with a growing population, Israel heavily invested in desalination by building five seawater desalination plants over the past two decades, combining for a total capacity of 585 million cubic meters (MCM) (Shemer and Semiat, 2017). In total, the sources in the INWSS consist of seawater desalination plants, brackish water desalination plants, aquifers, and Lake Kinneret (Mekorot, Israeli National Water Company, 2022). The system demands include municipal and agricultural demands, environmental demands that consists of water discharged into the Jordan River to maintain sufficient flow, and transboundary demands to the Kingdom of Jordan to satisfy a water supply contract between the two countries (Elmusa, 1995). A schematic of the INWSS is displayed in Fig. 1.

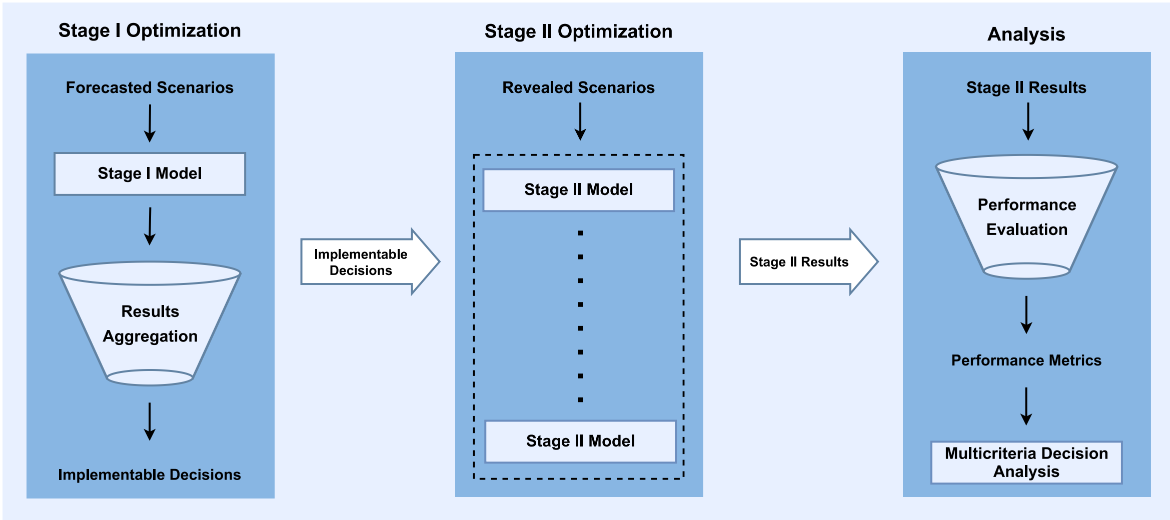

Fig. 2. Model framework comprised of a two-stage optimization approach followed by multicriteria decision analysis.

Despite the diversified water supply portfolio, Israel still faces the continual threat of water scarcity in its natural resources, where increased variability in future climate conditions is expected to exacerbate water stress (Gophen et al., 2020; Givati et al., 2019). Furthermore, over-extraction of groundwater aquifers allows for greater seawater intrusion (Housh, 2011) while both over-pumping and high evaporation levels are primary factors in the increasing salinity levels of Lake Kinneret (Rimmer et al., 2011). As such, it is necessary to properly manage the supply from desalination plants to blend with the high-salinity water from the natural resources in order to satisfy the demand and water quality requirements of the INWSS, all while maintaining sustainable water levels in the natural resources. During the water management planning process, the quantity of water produced from the desalination plants is decided in advance through contracts between plant managers and the water authority (Israeli Ministry of Finance, 2022), resulting in asynchronous decision timelines between the desalination plants and natural resources. When planning the water supply from each source, water managers must use forecasts of uncertain hydrological inflow to the natural resources and consumer demands in the system (Herman et al., 2014). However, a problem arises when the revealed inflows and demands deviate from their forecasted values and the desalination plants are constrained to the flow rate contracts. It is thus necessary to incorporate uncertainty in the inflows and demands into the decision-making process.

Previous studies have been conducted on management of the INWSS, including a focus on the blending of the multi-quality sources using a deterministic approach (Housh et al., 2012), a stochastic approach to managing uncertain aquifer recharge (Housh et al., 2013), and a robust approach to managing uncertain inflow to Lake Kinneret (Housh and Aharon, 2021). In the proposed model, the previous studies are expanded through the inclusion of both hydrological and demand uncertainties, implementation of a two-stage modeling framework, and evaluation of modeling results using a multicriteria decision analysis. These additions serve to provide a more complete description of the uncertainties faced by the INWSS, adapt the uncertainty management approach to account for the reality of asynchronous decision timelines faced by decision-makers, and present a comprehensive assessment of the inherent tradeoffs in the system that directly incorporates stakeholder preferences.

2.1.2. Optimization model

The proposed framework (see Fig. 2), comprised of a two-stage optimization model with a posteriori multicriteria decision analysis, was developed for the INWSS to determine the flow rates from the desalination plants that maximize stakeholder goals under a range of potential hydrological and demand scenarios. In the two stage optimization model, the management decisions are split into implementable and recourse decisions. The implementable decisions represent the flow rates supplied from the desalination plants and the recourse variables represent the flow rates supplied from the aquifers and Lake Kinneret, the water distribution and salinity levels in the supply system, and the water level in Lake Kinneret. In Stage I of the two-stage optimization process, the desalination flow rates are optimized with respect to N_0 of different forecasts of hydrological and demand scenarios, and the resultant set of desalination flow rates is aggregated into a family of N_1 sets of desalination flow rates that are representative of the full range of original solutions. In Stage II, each set of desalination flow rates is implemented as an input and the optimization model is solved for a new set of N_2 scenarios, allowing the recourse decisions to adapt to the revealed uncertainty. The Stage II model relaxes constraints from the Stage I model, allowing the recourse decisions to incur a deficit in supply at the demand zones, exceed salinity thresholds, and drop below the minimum sustainable water level in Lake Kinneret. Following the two stage process, the $N_1 \times N_2$ outputs of the Stage II model are distilled into N_1 sets of cost and robustness performance metrics, where the latter defines the extent to which the recourse decisions are able to withstand violating the demand, salinity, and sustainability constraints for uncertain scenarios for which they were not optimized for in the first stage. Further details on the calculation of the robustness metrics are provided in Section 2.4. To determine tradeoffs between the N_1 sets of performance metrics, the MCDA method PROMETHEE II (Preference Ranking Organization Method for Enrichment Evaluation) is utilized (Brans and De Smet, 2016).

2.2. First stage model

In the first stage, a nonlinear optimization model is formulated to determine the least-cost water supply mix for the INWSS for a set of hydrological and demand scenarios. The INWSS is modeled as a graph representing the system topology, where the nodes include the supply sources, demand zones, and intermediate junctions, and the edges represent the system links. The supply system is represented in Fig. 1, where the sources include five seawater desalination plants, two brackish water desalination plants, 13 aquifer pumping stations, and Lake Kinneret, which all blend together through the conveyance network to supply consumers represented through four municipal demand zones designated as Galilee West, North, Center, and South. Additionally, Lake Kinneret supplies water directly to the agricultural, environmental, and transboundary demand zones which represent local agricultural regions, the Jordan River, and the Kingdom of Jordan.

The decision variables in the first stage are decided for each month of time horizon $t = 1, \ldots, T$. The variables include the flow rates delivered to the system from the desalination plants Q_d^t, aquifers Q_a^t, and Lake Kinneret Q_k^t, the flow rates Q_ℓ^t and salinity levels C_ℓ^t for each link in the system, the flow rate Q_s^t and salinity levels C_s^t for the water discharged to the Jordan River, the flow rate Q_z^t and salinity levels C_z^t for the demand zones, and the salinity level C_k^t and water level H_k^t in Lake Kinneret. The inputs to the model include the salinity levels of the desalinated C_d^t and aquifer C_a^t water supplied to the system, the flow rates for the demand zones $\widetilde{D}_z^t$, the inflow into Lake Kinneret $\tilde{I}_k^t$, the mass of solute into Lake Kinneret M_k^t, and the initial salinity C_k^0 and water level H_k^0 in Lake Kinneret.

The constraints of the optimization model include mass and salinity balances at the intermediate junctions i and demand zones z, complete-mixing at the intermediate junctions and demand zones, and state equations that track salinity and storage in Lake Kinneret. The general equations for the mass and salinity balances in each month t are formulated as follows:

$$\sum_{\ell \in L_{in,z}} Q_\ell^t - \sum_{\ell \in L_{out,z}} Q_\ell^t = \widetilde{D}_z^t \qquad t = 1, \ldots, T \tag{1}$$

$$\sum_{\ell \in L_{in,z}} C_\ell^t Q_\ell^t - C_z^t \sum_{\ell \in L_{out,z}} Q_\ell^t = C_z^t \widetilde{D}_z^t \qquad t = 1, \ldots, T \tag{2}$$

where $L_{in,z}$ and $L_{out,z}$ are the sets of links into and out of demand zone z, and $\widetilde{D}_z^t$ is the uncertain demand at demand zone z. When Eqs. (1) and (2) are applied to the intermediate junctions, the terms C_z^t and $\widetilde{D}_z^t$ on the right-hand side of the mass and salinity balance constraints are zero. The blending of water in each node is modeled as complete and instantaneous mixing (Loucks and Van Beek, 2017):

$$C_i^t = \frac{\sum_{\ell \in L_{in,i}} C_\ell^t Q_\ell^t}{\sum_{\ell \in L_{in,i}} Q_\ell^t} \qquad t = 1, \ldots, T \tag{3}$$

where $L_{in,i}$ is set of links flowing into node i. Mass and salinity balances are also applied at Lake Kinneret, where Eq. (4) models the water mass balance, Eq. (5) models the solute mass balance, and Eq. (6) models the relationship between the water level and storage volume:

$$S_k^t - S_k^{t-1} + Q_k^t = \tilde{I}_k^t \qquad t = 1, \ldots, T \tag{4}$$

$$C_k^t \cdot S_k^t - C_k^{t-1} \cdot S_k^{t-1} + C_k^t \cdot Q_k^t = M_k^t \qquad t = 1, \ldots, T \tag{5}$$

$$S_k^t = aH_k^t + b \qquad t = 1, \ldots, T \tag{6}$$

where Q_k^t is the flow from Lake Kinneret to the rest of the system, S_k^t is the storage volume, H_k^t is the water level, C_k^t is the salinity, $\tilde{I}_k^t$ is the uncertain hydrological input, M_k^t is the total solute mass input, and a and b are parameters that approximate the relationship between the storage and water level (Housh et al., 2012). Eqs. (4) and (5) are the state equations that link variables through time steps t and $t-1$.

Upper and lower bounds are placed on the decision variables that represent operational constraints in the INWSS and enforce the goals of Israel Water Authority (IWA) to supply consumers with high-quality water and maintain sustainable water levels in Israel's natural resources. The desalination flow rates are limited by the maximum monthly capacity of each plant. To meet water quality standards for the consumers, maximum limits are placed on the salinity variables at the demand zones. The lower limit for all flow rate and salinity variables is zero unless previously specified otherwise. To ensure sustainable usage of the natural resources, the monthly extraction flow rate from the aquifers and Lake Kinneret are limited by an upper bound, a minimum discharge from Lake Kinneret to the Jordan River is applied to maintain environmental flows, and the water level in Lake Kinneret is bounded by a lower and upper limit to avoid over-extraction and overfilling. Lake Kinneret is below sea level, and the lower limit is set at the historical minimum level of −214.87 m, while the upper limit is set as at −208.8 m.

The objective function for the Stage I model combines the operational cost of supply water from each source with sustainability objectives set by the decision-maker. The operational costs include the unit cost of water supply from desalination plants and aquifers, and dynamic tariffs that represent the energy cost of pumping from Lake Kinneret for different seasons and supply amounts. The sustainability objectives are represented through variable rates imposed on discharge to the Jordan River and extraction from Lake Kinneret, where the rate per unit of water changes based on the quantity of water discharged or extracted. The objective function is formulated as:

$$\text{minimize} \quad \sum_t \left(\sum_d r_d Q_d^t + \sum_a r_a Q_a^t + f_1(Q_k^t) \right) + f_2(Q_s^T) + f_3(Q_k^T) \tag{7}$$

where Q_d^t, Q_a^t, Q_k^t represent the flow rate supplied from desalination plants, aquifers, and Lake Kinneret at time t, Q_s^T and Q_k^T represent the total quantity of water discharged into the Jordan River and supplied from Lake Kinneret over the entire time horizon, r_d and r_a represent the unit costs applied to desalination plants and aquifers, and f_1^t, f_2, and f_3 are functions that represent complex cost structures for the supply sources and sustainability considerations for Israel's natural resources. In addition to the cost functions included in Eq. (7), arbitrarily small unit costs are applied to the conveyance through one of the links in each pair of bidirectional links seen in Fig. 1, thereby ensuring conveyance in only one direction. The three functions f_1^t, f_2, and f_3 are displayed in Fig. 3. Fig. 3(a) shows f_1^t, a piecewise linear function that models the energy cost of pumping from Lake Kinneret, represented through dynamic tariffs. The y-axis is represented by the total cost of pumping, slope of each line segment represents the tariff applied depending on the month t and quantity of water extracted Q_k^t, and the three separate lines represent the different cost structures applied during the winter (blue), summer (orange), and remaining months (yellow). Fig. 3(b) shows f_2, a piecewise damage function that represents the desire to avoid discharging large quantities of water from Lake Kinneret into the Jordan River. The y-axis represents the total cost of discharging water to the Jordan River and the x-axis represents the total quantity of discharged water throughout the year. At low discharge levels represented in the first segment, no cost is applied to the objective function, and at high discharge levels represented by the second segment, a penalty cost is applied to the objective. Fig. 3(c) shows f_3, a nonlinear cost function that represents the sustainability goal of limiting pumping from Lake Kinneret. As opposed to f_1^t, f_3 does not represent a cost incurred from pumping, but rather, it is a quadratic damage function that makes the cost of withdrawing water from Lake Kinneret more expensive as the total amount of water withdrawn increases. The y-axis represents the total cost of withdrawing water and the x-axis represents the total amount of water withdrawn from Lake Kinneret throughout the year. For all functions, the costs are in Million New Israeli Shekels (MNIS) and the flow rates are in MCM.

The objective function in Eq. (10) is converted to a linear function in order to decrease the computational complexity of the model. First, the quadratic cost function f_3 is approximated as a piecewise linear function (Housh and Aharon, 2021):

$$f_3(Q_k^T) \approx \hat{f}_3(Q_k^T) = \max_{s=1\ldots S} (a_s Q_k^T + b_s) \tag{8}$$

where S is the number of segments in $\hat{f}_3$. Each piecewise function is then formulated as a linear program:

$$\begin{aligned} \min \quad & \lambda \\ \text{s.t.} \quad & a_s Q + b_s \le \lambda \qquad s = 1, \ldots, S \end{aligned} \tag{9}$$

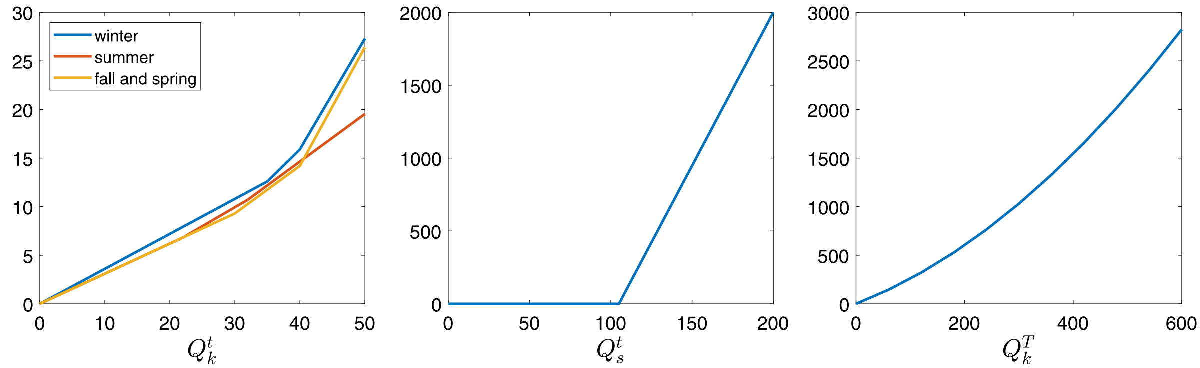

Fig. 3. Cost functions.

where Q is a generic flow rate variable and λ is an auxiliary variable that represents the value of the piecewise function. The formulation in Eq. (9) is applied to f_1 and f_2 for all t where $Q = Q_k^t$ and $Q = Q_s^t$, respectively, and applied to f_3 where $Q = Q_k^T$. The final objective function is formulated as:

$$F_1 = \text{minimize} \sum_t \left(\sum_d r_d Q_d^t + \sum_a r_a Q_a^t + \lambda_1^t + \lambda_2^t \right) + \lambda_3 \tag{10}$$

where λ_1^t, λ_2^t, and λ_3 are the auxiliary variables representing the values of f_1, f_2, and f_3.

The uncertain inputs $\widetilde{D}_z^t$ and $\widetilde{I}_k^t$ are sampled from a joint inflow-demand multivariate normal distribution, characterized by a mean vector $\boldsymbol{\mu}$ and covariance matrix $\boldsymbol{\Sigma}$. The values of the mean vector are populated by the expected inflow and demand values for each month (referred to as the baseline scenarios in the remainder of the text). The baseline scenario for the consumer demands are provided by the IWA based on extrapolation of historical demand records, population growth predictions, and analysis of future development plans (Israel Water Authority, 2011). The baseline hydrological scenario is based on the combination of expected direct inflows from a local stream, surface flow from the surrounding basin, percolation into the subsurface, and evaporation values, and is provided by the IWA in an internal report. The diagonal of the covariance matrix is populated by the variance of each parameter and the off-diagonal cells are populated by the pairwise covariance values between each of the parameters. Each covariance value is calculated from the pairwise correlations and standard deviation of each parameter. The correlation values are characterized by two variable relationships, the correlation between inflows in different months ($\rho = 0.7$) and the correlation between demands in different months ($\rho = 0.7$). While a correlation between inflow and demand is also expected, no correlation was assumed in order to sample a larger range of uncertainty scenarios. The standard deviation for the inflows in each month are set at 10% of the baseline annual inflow ($\sigma_k^t = 10\,MCM$) and the standard deviations for the demands are set at 10% of each baseline demand ($\sigma_z^t = 0.1 D_z^t$). Furthermore, the Latin Hypercube Sampling algorithm was used for the sampling procedure in order to increase the diversity of the input scenarios (Rajabi et al., 2015).

For each realization of $\widetilde{D}_z^t$ and $\widetilde{I}_k^t$, the first stage model is solved, generating a large set of implementable decisions. The set of implementable decisions is then aggregated into a smaller subset of decisions using the k-medoids algorithm, where the medoid of each cluster populates the final subset of implementable decisions (Arora et al., 2016). The aggregation process serves to remove redundant implementable decisions, increase the variety between decisions, and decrease the total computation time required for the full two-stage optimization model (Housh et al., 2013). While many clustering algorithms can be applied to aggregate the set of implementable decisions, the k−medoids algorithm is selected to ensure the new subset of implementable decisions is comprised of values from the original set. The use of algorithms that select the centroid of the cluster may result in infeasibilities in the optimization model, since the implementable variables would not have been actual solutions determined from the Stage I model. The final result of the clustering process is a family of N_1 sets of implementable decisions, where an individual set is denoted by Q_D.

2.3. Second stage model

Following the aggregation of the implementable decisions, each set Q_D is provided as an input into the Stage II model and the model is solved for N_2 more realizations of $\widetilde{D}_z^t$ and $\widetilde{I}_k^t$. The total number of model runs in the second stage is thus $N_1 \times N_2$. In the second stage, the model described in Section 2.2 is relaxed to allow the system to incur a deficit to the demand zones, exceed the salinity limits at the demand zones, and violate the water level limits in Lake Kinneret. The changes reflect the IWA goals of meeting all demands, supplying high-quality water to consumers, and maintaining sustainable water levels in Lake Kinneret. To allow demand deficits, Eqs. (1) and (2) which represent the general form of the water and solute mass balances, are relaxed for the demand zones:

$$\sum_{\ell \in L_{in,z}} Q_\ell^t - \sum_{\ell \in L_{out,z}} Q_\ell^t \le \widetilde{D}_z^t \qquad t = 1, \dots, T \tag{11}$$

$$\sum_{\ell \in L_{in,z}} C_\ell^t Q_\ell^t - C_z^t \sum_{\ell \in L_{out,z}} Q_\ell^t \le C_z^t \widetilde{D}_z^t \qquad t = 1, \dots, T \tag{12}$$

Next, the upper bounds on C_z^t and the lower bound on H_k^t are removed, allowing the salinity at the demand zones and the water level in Lake Kinneret to exceed the limits set by the IWA. A violation occurs when the model fails to supply all demands, exceeds the salinity limits, or exceeds the water level lower limit. Penalty functions are added to the objective function that penalize each of the constraint violations, where the demand, salinity, and sustainability violations are calculated as:

$$v_d = \sum_z \sum_t \left(\widetilde{D}_z^t - Q_z^t \right) \tag{13}$$

$$v_q = \sum_z \sum_t \max \left(0, C_z^t - \overline{C}_z \right) \tag{14}$$

$$v_s = \sum_t \max \left(0, \underline{H}_k - H_k^t \right) \tag{15}$$

where Q_z^t is the demand supplied to demand zone z and is equivalent to the left-hand side of Eq. (11), $\widetilde{D}_z^t$ is the uncertain demand at demand zone z, $\overline{C}_z$ is the upper limit for salinity at demand zone z, and $\underline{H}_k$ is the water level lower limit in Lake Kinneret. The demand violation v_d represents the deviation between the demand and actual water supplied, where Q_z^t cannot supply more water than $\widetilde{D}_z^t$. However, in Eqs. (14) and (15) where C_z^t and H_k^t are unbounded, violations are only considered when the deviations exceed the upper and lower limits, respectively. Thus, v_q and v_s are formulated such that the violations are only counted when the deviations are positive, i.e., when $C_z^t > \overline{C}_z$ and

$H_k^t < \underline{H}_k$ (Boyd et al., 2004). The violations are formulated as penalty functions and added to the objective function in the first stage Eq. (10) to yield the final objective function for the second stage model:

$$F_2 = \text{minimize} \quad \sum_t \left(\sum_d r_d Q_d^t + \sum_a r_a Q_a^t + \lambda_1^t \right) + \lambda_2 + \lambda_3 + \alpha_d v_d + \alpha_q v_q + \alpha_s v_s \tag{16}$$

where α_d, α_q, and α_s are the penalty coefficients for each respective function. The final outputs of the two stage model are N_1 sets of implementable decisions and N_2 sets of recourse decisions for each set of implementable decisions.

2.4. Model evaluation

The performance metrics used to assess the Stage II solutions are the desalination cost I_{DC}, expected recourse cost I_{RC}, expected total cost I_{TC}, and robustness with respect to demand I_{RD}, quality I_{RQ}, and sustainability I_{RS}. The units for all cost metrics are MNIS whereas the robustness metrics are unitless. Each metric is a vector of length N_1, where each index n represents a different Stage I realization. Both the total cost and recourse costs are $N_1 \times N_2$ matrices, where each value in the total cost matrix is calculated as the objective function in the Stage I model F_1 described in Eq. (10), and each value in the recourse cost matrix is calculated as:

$$F_{RC} = \sum_t \left(\sum_a r_a Q_a^t + \lambda_1^t + \lambda_2^t \right) + \lambda_3 \tag{17}$$

where F_{RC} is the combined cost of supply from the aquifers and Lake Kinneret, and discharge to the Jordan River. The cost metrics I_{TC} and I_{RC} are then calculated by averaging each row of the total and recourse cost matrices over all Stage II runs, resulting in vectors I_{TC} and I_{RC} of size N_1.

Robustness has been defined in water systems planning as the ability of a water resource system to maintain performance under a wide range of possible future conditions (Borgomeo et al., 2018). For this research, the definition of robustness is adapted to reflect system performance against different realizations of $\widetilde{D}_z^t$ and $\widetilde{I}_k^t$. In this definition, system performance is equated with the violations of the demand, quality, and sustainability constraints as calculated in Eqs. (13)–(15), and as such, the robustness metrics are calculated from each v_1, v_2, and v_3. To account for both the magnitude and frequency of violations, the robustness metrics are formulated as the combination of (1) the average normalized magnitude of violations (Abokifa et al., 2020) and (2) the percent of Stage II solutions that incur a violation (Whateley et al., 2014; Moody and Brown, 2013). For each Stage I solution, the final demand, quality, and sustainability metrics are calculated as:

$$I_{RD}(n) = \left(1 - \frac{1}{N_d} \sum_{i=1}^{N_2} \frac{v_d^i}{\max_i(v_d^i)} \right) \cdot p_d \tag{18}$$

$$I_{RQ}(n) = \left(1 - \frac{1}{N_q} \sum_{i=1}^{N_2} \frac{v_q^i}{\max_i(v_q^i)} \right) \cdot p_q \tag{19}$$

$$I_{RS}(n) = \left(1 - \frac{1}{N_s} \sum_{i=1}^{N_2} \frac{v_s^i}{\max_i(v_s^i)} \right) \cdot p_s \tag{20}$$

where n is the index of the Stage I solution, N_d, N_q, and N_s represent the total number of violations of each constraint across all Stage II solutions, and p_d, p_q, and p_s represent the fraction of Stage II solutions that have at least one violation. The scaling parameter is selected as the maximum violation across all Stage II solutions for each constraint in order to convert all of the robustness metrics into a value between 0 and 1. The average normalized violations are then subtracted by 1 in order to equate a value of 1 to maximum robustness, and a value of 0 to minimum robustness.

2.5. Multicriteria decision analysis

In the first step of the Stage II model evaluation, the $N_1 \times N_2$ sets of recourse decisions are distilled into N_1 sets of six performance metrics. While the performance metrics provide a comprehensive representation of the Stage II results, evaluating tradeoffs between the solutions is challenging when there are six different criteria and many solutions. To aid decision makers in identification of the decision alternative most aligned with their preferences, the MCDA method PROMETHEE II is utilized to filter and rank the sets of solutions against one another based on the performance metrics (Brans and De Smet, 2016). Intuitively, the PROMETHEE method involves evaluating and comparing the different solutions, where the decision-makers' preferences are included by assigning weights to the different metrics. The final results are an aggregation of a solution's performance across all metrics into a single score that reflects the alignment of the solution with the decision-makers preferences. A summary of the process is illustrated in Fig. 4. In step (a), the deviation between each pair of solutions is calculated for a performance metric k:

$$d_k(i,j) = I_k(i) - I_k(j) \tag{21}$$

where i and j represent the different decision alternatives. In step (b), a preference function P_k is defined which indicates the extent to which a solution i outranks or is outranked by a solution j, where the outranking score is between 0 and 1. For the selected preference function, d_k^{min} represents the minimum deviation value below which a preference score of 0 is assigned, d_k^{max} represents the maximum deviation value above which a preference score of 1 is assigned, and any d_k between the two limits is linearly interpolated between 0 and 1. Various preference functions can be chosen, however, the preference function in (b) is selected to ignore small difference in performance and avoid over-valuing large difference in performance. In step (c), the overall preference index π is calculated through a weighted summation of all the preference scores:

$$\pi(i,j) = \sum_{k=1}^{6} w_k P_k(i,j) \tag{22}$$

where weights w_k are values between 0 and 1 that represent stakeholder relative preferences between the different performance metrics. In step (d), positive and negative outranking flows for each alternative i, ϕ^+ and ϕ^-, are determined by averaging the columns and rows of π for all $i \neq j$, formulated as:

$$\phi_i^+ = \frac{1}{N_1 - 1} \sum_{j \in A}^{N_1} \pi(i,j) \tag{23}$$

$$\phi_i^- = \frac{1}{N_1 - 1} \sum_{j \in A}^{N_1} \pi(j,i) \tag{24}$$

where A is the set of decision alternatives to i, column i of π represents the extent to which solution i outranks the other solutions, and row i of π represents the extent to which solution i is outranked by the other solutions. The final score for each solution is then calculated as the net outranking flow:

$$\phi_i = \phi_i^+ - \phi_i^- \tag{25}$$

Following the application of the PROMETHEE II outranking method to the performance metrics, the decision alternative with the highest value is denoted as the favored choice for the given preferences.

3. Results

The proposed methodology is applied to the INWSS where the uncertain hydrological inflows and consumer demands threaten the capability of water managers to ensure all demand, quality, and sustainability requirements are met. The goal of this analysis is to first

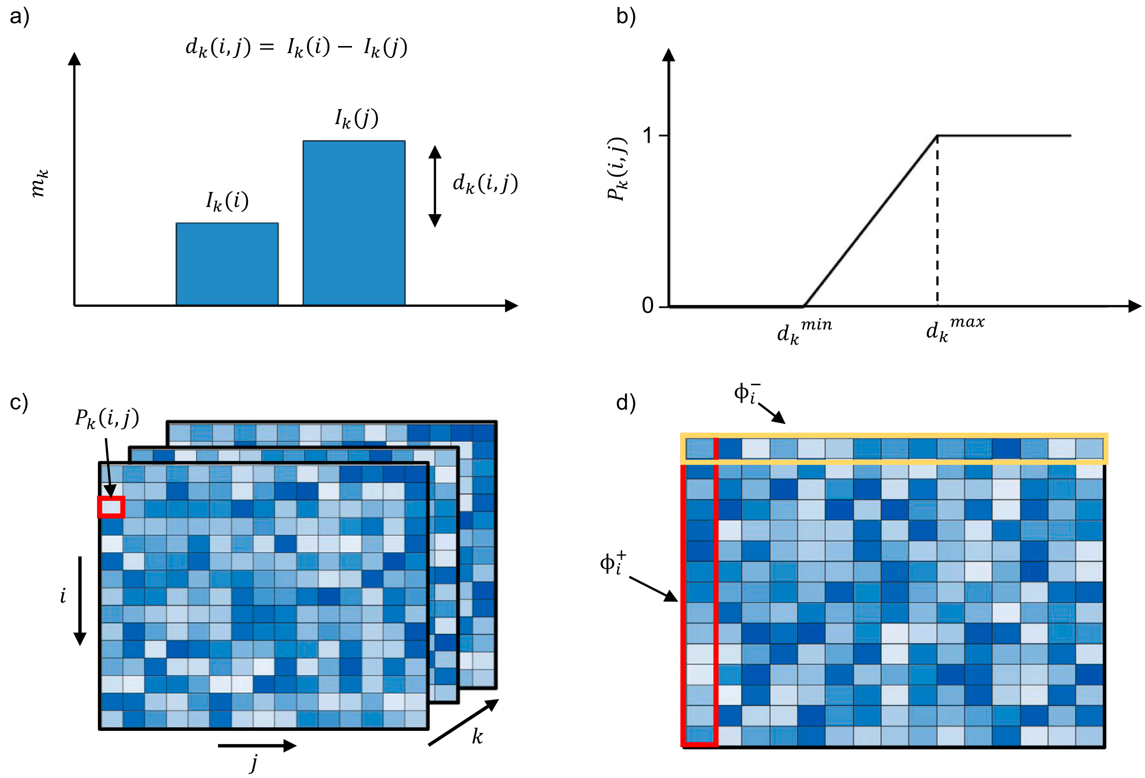

Fig. 4. PROMETHEE II methodology.

determine the extent to which the implementable decisions can prepare the system for various realizations of uncertainty, and then elucidate the tradeoffs between different decisions with regard to operational cost and system robustness. The results of the research are summarized as follows. First, the Stage I results for the baseline hydrological and demand scenarios, where the outputs represent the deterministic INWSS model when no consideration is given to uncertainty are presented. Next, the robustness of the system is calculated by introducing new scenarios in the Stage II model for which baseline implementable decisions were not originally optimized for. The full implementation of the modeling framework is then applied, in which $N_0 = 1000$ realizations of the Stage I model are solved, the implementable decisions are clustered into $N_1 = 20$ representative sets, and each set is implemented into the Stage II model and tested against $N_2 = 50$ new scenarios. Tradeoffs between the individual cost metrics I_{DC}, I_{RC}, and I_{TC} are then examined from the Stage II results, and the PROMETHEE II method is applied to incorporate all performance metrics into a single comparative analysis that reveals tradeoffs between the operational cost and system robustness.

Implementation of the proposed framework, including mathematical model development, scenario sampling, multicriteria assessment, and all other data analysis, was performed using MATLAB, and the optimization model was solved with the global optimization solver BARON (Sahinidis, 2017). All data to model the INWSS is available in the Supplementary Material. The proposed model was developed through a collaboration with the IWA, which gave feedback for the abstraction of the model and its assumptions (Housh, 2011). Model validation was conducted through extensive sensitivity analyses, wherein the model was tested against extreme values of key parameters such as water inflow rates, salinity levels, and costs, and examined to ensure the model responded as expected. Further validation was performed on the results, namely, water and solute mass balance checks on individual nodes, the Lake Kinneret sub-system, and the system in its entirety.

3.1. Stage I baseline performance

In this section, the outputs of the Stage I model are analyzed, where the inputs are the baseline scenarios for the hydrological inflow and consumer demands. The purpose of this analysis is to examine the results of the optimization model applied to the INWSS when the model has perfect foresight of the uncertainty. The baseline hydrological inflow and the baseline demands for the four municipal zones are displayed as the black lines in Fig. 5(a) and (b), respectively. In Fig. 5(a), the baseline inflow scenario provides Lake Kinneret with a net total 103 MCM over the entire year, however, the inflow is negative from June until October. Such negative inflow values occur when evaporation into the atmosphere and percolation into the subsurface exceed stream and surface flows, resulting in net water loss. The months with negative inflow coincide with months with high demands in the municipal demand zones, as shown in Fig. 5(b).

The results of the Stage I model are summarized in Figs. 6 and 7. Fig. 6(a) displays the flow rates supplied in each month from the desalination plants, aquifers, and Lake Kinneret and (b) the monthly water levels in Lake Kinneret. Fig. 7 displays the average salinity level in the demand zones in (a), and the monthly salinity levels in Lake Kinneret in (b). The model outputs displayed in both figures represent the deterministic condition, where the inputs are the baseline scenario in which no uncertainty is considered. Since the Stage I model has complete knowledge of the hydrological and demand conditions, the supply flow rates and water allocations in the system are able to be determined such that all demand, salinity, and sustainability goals are met.

In Fig. 6(a), the flow rates supplied from the three sources, indicated by the darker color of each bar, are plotted over the respective monthly capacities, indicated by the lighter color in each bar. In the summer months of July–August, all three sources provide an increase in supply and the aquifers in particular reach full utilization in order to meet the seasonal high demands shown for each of the municipal consumers in Fig. 5(b). As the extraction levels from Lake Kinneret rise during

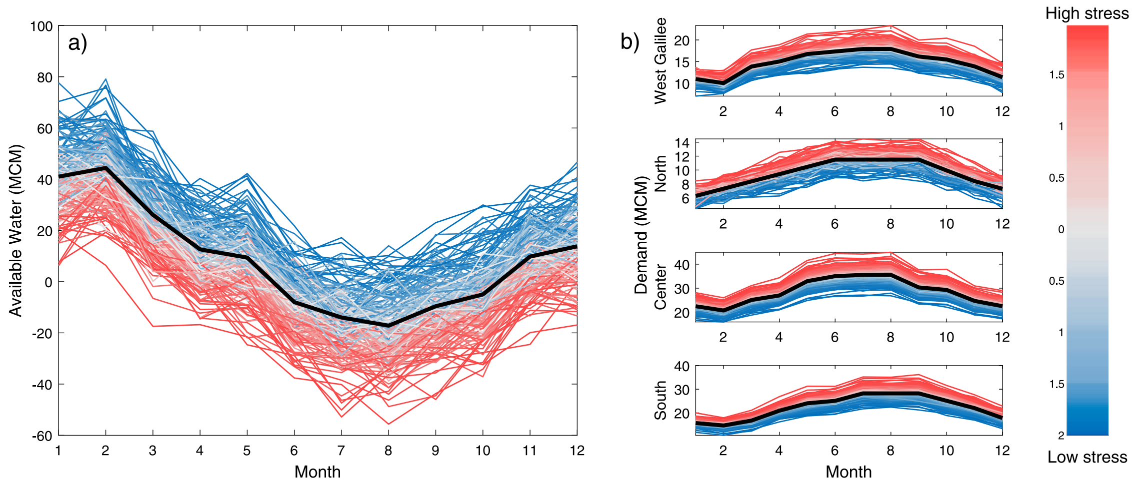

Fig. 5. Baseline hydrological and demand scenarios input to Stage I model (black line), and 200 realizations of $\widetilde{I}$ and $\widetilde{D}$ input to Stage II model (colored lines).

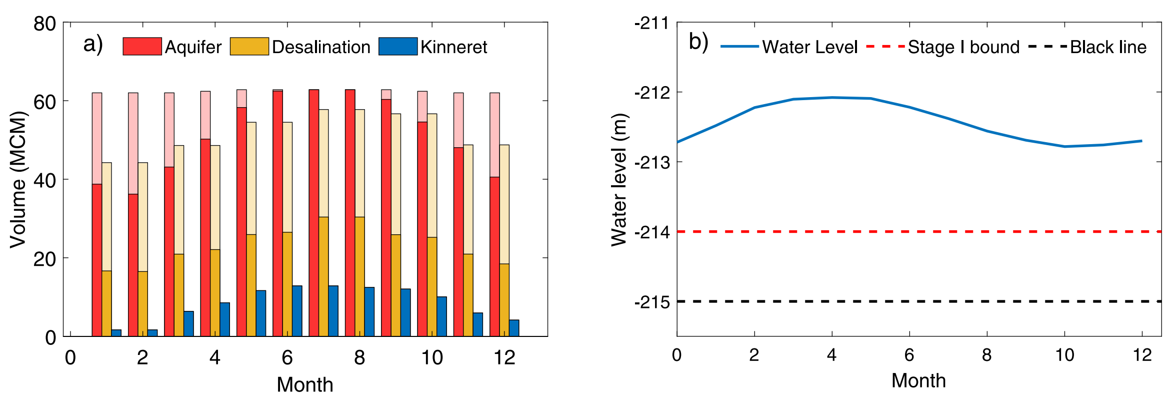

Fig. 6. Baseline scenario results: (a) monthly supply flow rates from each water source, (b) monthly water levels in Lake Kinneret.

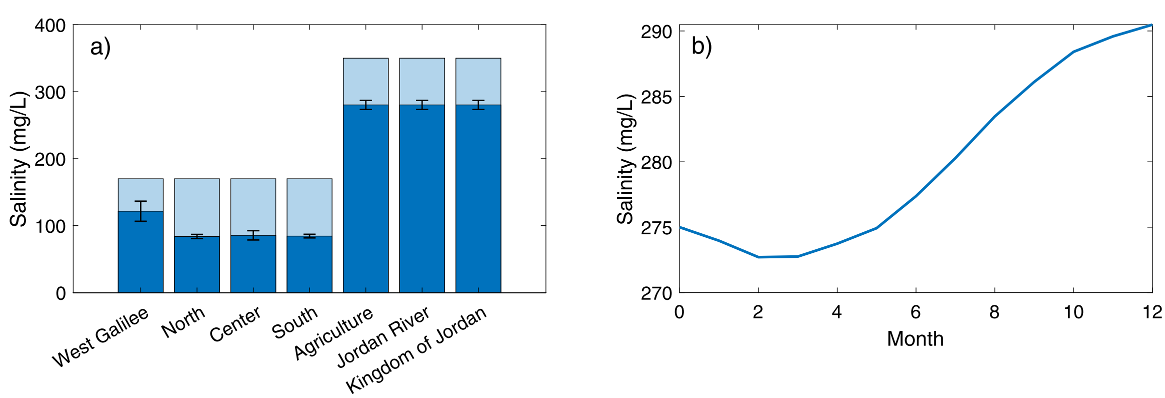

Fig. 7. Baseline scenario results: (a) average salinity of supply for demand zones, (b) monthly salinity levels in Lake Kinneret.

these months, the outflow exceeds the inflow and the water level begins to drop, as shown in Fig. 6(b) where the lake water level is plotted along with the lower boundaries. The lower of the two bounds is designated as the "black line" by the IWA and indicates the lowest level in the historical record, while the red boundary represents the boundary imposed on H_k^t in the Stage I model. In the baseline scenario, the water level in Lake Kinneret does not threaten to cross the Stage I bound.

In the baseline scenario, Lake Kinneret does not need to supply any water to the municipal demand zones, but rather, all water from the lake is distributed directly to the local demand zones represented by the agricultural region, the Jordan River, and the Kingdom of Jordan. The water usage for these three demand zones has a much higher salinity threshold than the municipal demand zones, which allows them to utilize water directly from Lake Kinneret without any mixing from other sources. Fig. 7(a) displays the average salinity level for the year for each demand zone, indicated by the dark blue bars, over the allowable salinity levels, indicated by the light blue bars. West Galilee is generally more prone to high salinity levels due to its reliance on water from Lake Kinneret and local aquifers to meet demand, however,

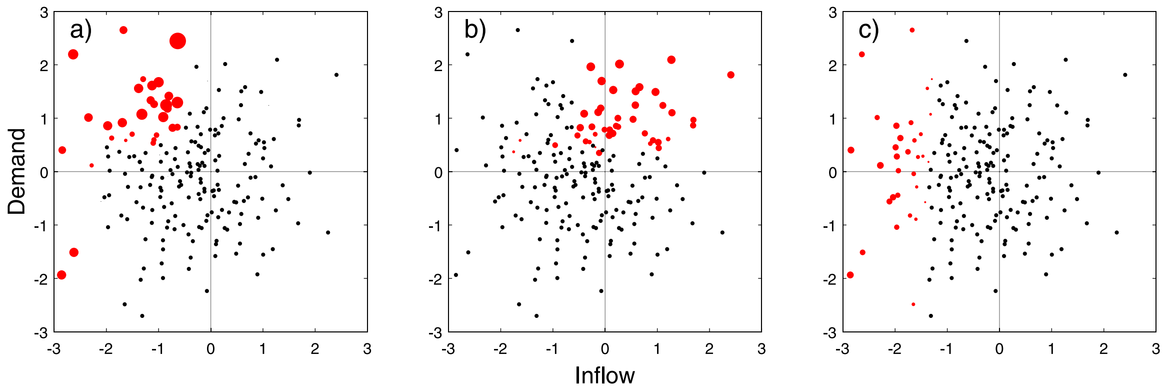

Fig. 8. Constraint violations in baseline solution for 200 uncertain hydrological and demand scenarios in Stage II: (a) demand, (b) water quality, and (c) sustainability.

it primarily receives supply from aquifers in the baseline scenario which allows the demand zone to remain within allowable salinity levels. The remaining consumers zones have much greater access to the seawater desalination plants which results in low salinity levels. The salinity levels for the agriculture region, Jordan River, and Kingdom of Jordan are equal to the average salinity level in Lake Kinneret, where the monthly salinity values plotted in Fig. 7(b) show an increasing level of salinity throughout the year due to water loss and solute transport into the lake.

3.2. Stage II baseline performance

In this section, the implementable decisions optimized for the baseline scenario, i.e., the desalination flow rates in Fig. 6(a), are tested against 200 new hydrological and demand scenarios to assess the system performance when the uncertain inputs deviate from their expected values. Given the baseline implementable decisions, the recourse decisions are found for each of the new input scenarios, and the system performance for each scenario is assessed through violations of the demand, quality, and sustainability constraints. Fig. 5 displays the 200 new input scenarios for the hydrological inflow to Lake Kinneret in (a), and the municipal demands in (b). The environmental, agricultural and transboundary demands are not subject to uncertainty, as the local agricultural regions and Kingdom of Jordan have fixed supply agreements with the IWA, and the environmental flows into the Jordan River are governed by minimum supply constraint and the objective function. For all plots, the baseline scenario is the black line, and the sampled scenarios are colored based on their standardized annual values. The process of standardizing the data allows the two inputs to be compared with one another, as they are now defined by their standard deviations with respect to their probability distribution as opposed to being defined by their original units. Additionally, the standardized scores are given as absolute values on the color bar, where scenarios that induce high stress in the system are indicated by red, i.e., low $\widetilde{I}$ and high $\widetilde{D}$, and scenarios that induce low stresses in the system are indicated by blue. Preliminary analysis of the Stage II model revealed a tradeoff under high-stress scenarios in the decision to either incur penalties for supply deficits or pay increasing rates for supply from Lake Kinneret, however, the penalties applied to quality and sustainability violations were shown to be redundant. As a result, the penalty coefficients for the quality and sustainability violations in the Stage II model were set at 0 for the application to the INWSS.

In Fig. 8, the violations with respect to the three metrics are displayed as scatter plots, where each individual point represents a single iteration of the Stage II model. The red markers on each plot represent the Stage II solutions in which there was at least one violation with respect to the specific robustness metric explored, and the black markers represent Stage II solutions in which there were no violations. Additionally, the size of the red markers represents the normalized sum of the violation magnitudes. The x and y axes represent the mean hydrological inflow and demand inputs across the year, respectively, where the values are standardized such that the origin represents the baseline hydrological and flow scenarios, the location of each point on the grid represents the number of standard deviations away from the baseline scenario each input lies. For example, in Fig. 8(a), there are a total of 200 markers that each represent a Stage II solution. The first quadrant represent solutions that were solved for high inflows and high demands, and similarly, the points in the third quadrant represent solutions that were solved for low inflows and low demands. The red markers represent solutions that violated the demand constraints, and the size of each marker represents the extent of the violation. Likewise, the red markers in Fig. 8(b)–(c) represent violations in the quality and sustainability constraints.

Low hydrological input scenarios were the primary cause of supply and sustainability violations, as displayed in Fig. 8(a) and (c), where supply violations primarily occurred in scenarios with high demand in conjunction with low hydrological input. While salinity violations also correlated with high demand scenarios, they primarily occurred during periods of high hydrological input, as shown by the activity in the upper right quadrant of Fig. 8(b). In such a scenario, Lake Kinneret is sufficiently replenished to allow for a larger volume of available supply water as well as a lower rate for pumping. This combination of factors yields a greater utilization of supply water from Lake Kinneret which raises the salinity of the water delivered to nearby consumer zones past the allowable threshold. Any combinations of scenarios less than 0.3 standard deviations away from the baseline scenario do not incur any violations, indicating the baseline solution to be robust to small changes in the forecasted scenarios. However, Fig. 8(b) reveals a violation that occurs when the demand scenario exceeds 0.3 standard deviations, even when the inflow scenario is near the baseline value. Overall, only 56% of the solutions had zero violations. No violations are incurred when the revealed uncertainty is less severe than the hydrological and demand forecasts, as seen in the bottom right quadrant of the three plots.

3.3. Two-stage implementation

In this section, the full two-stage model was applied to analyze the performance of a range of different desalination flow rates against potential future scenarios. Cost and robustness metrics are calculated for each set of desalination flow rates following the Stage II model, and final results are analyzed to determine tradeoffs between the upfront cost of investing in desalination, and the expected recourse and total costs of system operation. First, the Stage I model was solved for $N_0 =$ 1000 realization of the uncertain scenarios, producing a total of 837 feasible sets of desalination flow rates. Since the Stage I model has strict bounds on demand, quality, and sustainability, a total of 163 of the input scenarios resulted in infeasible solutions. The 837 sets of

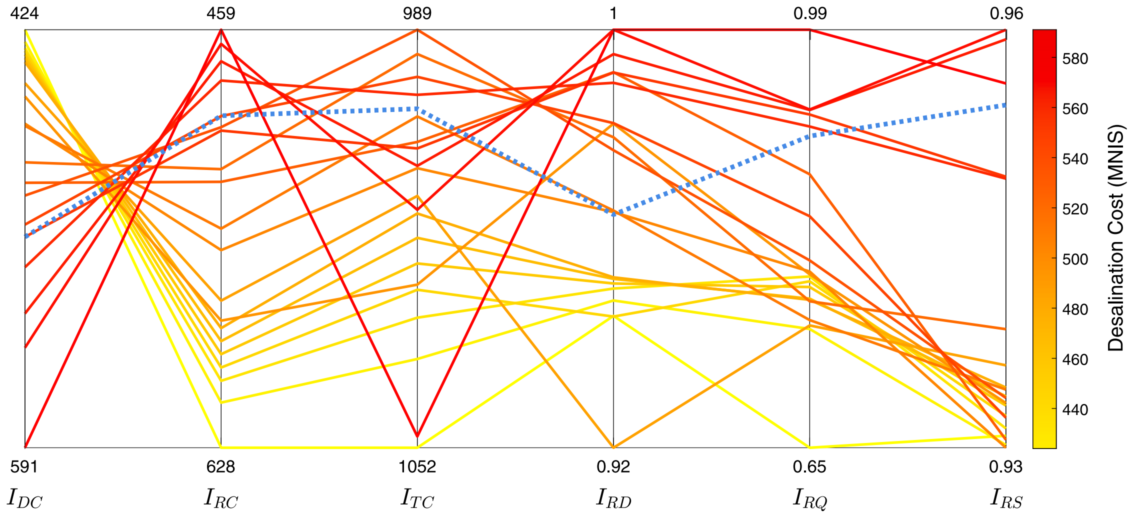

Fig. 9. Two-stage model results. The baseline solution is represented by the blue dashed line and all other lines are colored with respect to desalination cost.

desalination flow rates were then aggregated to $N_1 = 20$ unique sets of desalination flow rates (as detailed in Section 2.1.2). Next, the new decisions were passed to Stage II where they were each tested against $N_2 = 50$ new input scenarios. The performance of each of the new desalination decisions is plotted on parallel axes in Fig. 9, where the performance metrics are calculated as in Section 2.4. The x-axis of the plot shows the cost metrics I_{DC}, I_{RC}, and I_{TC} in units of MNIS, and the robustness metrics I_{RD}, I_{RQ}, and I_{RS} which are unitless. The y-axis shows the value of each performance metric for all desalination decisions determined from the Stage I model. For each axis, the value that represents the best performance, e.g., lowest cost and highest robustness, is found at the top of the axis, and the value that represents the worst performance is found at the bottom. Each line is colored with respect to its total cost of desalination, where red lines represent solutions that have a greater investment in desalination and yellow lines represent solutions that have lower investment in desalination. The performance of the baseline solution is plotted as the dashed blue line for comparison with the alternative solutions.

The intersecting lines indicate the presence of tradeoffs in system performance between the different solutions. Looking at the relationship between the connected values in the I_{DC} and I_{RC} axes, a clear tradeoff exists between the cost of desalination and the expected recourse costs, as indicated by the lines with high desalination cost also tending to have low recourse costs, and vice versa. This relationship suggests that a greater upfront investment in desalination reduces the potential recourse costs once the uncertainty has been revealed. A similar relationship holds between the desalination cost and the total operational cost, however, some solutions over-invest in desalination to the point at which it outweighs any savings accumulated in the recourse costs. The tradeoffs between the cost metrics apparent in Fig. 9 are made explicit in Fig. 10, where the desalination-recourse cost relationship is plotted in (a), and the desalination-total cost relationship is plotted in (b). It can be seen that as desalination investment increases, the range of potential costs once the uncertainty is revealed is diminished, i.e., paying more for desalination upfront limits the expected future costs and hedges against extreme outcomes.

3.4. Evaluation of decision alternatives

In this section, the PROMETHEE II method is applied to the set of N_1 performance metrics calculated from the set of N_1 implementable decisions and the subsequent Stage II recourse decisions. A sensitivity analysis is then performed on the stakeholder preferences, represented by the performance metric weights w_k, in order to assess the tradeoffs between operational cost and system robustness. The weights are first split into the two categories of cost and robustness, where each set of weights is represented by a single weight, w_C and w_R, divided equally within the category. The two representative weights are then varied between 0 and 1 over 50 iterations (step size = 0.02), where $w_C + w_R = 1$, and the PROMETHEE II analysis is repeated for each iteration. As the stakeholder preferences shift from a cost-focus ($w_c = 1$) to a robustness-focus ($w_R = 1$), the favored solution adapts to the new preference values. Fig. 11 displays the results of the sensitivity analysis, where Fig. 11(a) shows the upfront desalination cost versus the combined robustness score for the solutions that were included in the optimal set, and Fig. 11(b) shows the results of the two-stage model where the optimal solutions are highlighted and the base solution is displayed as a blue dashed line. The markers in Fig. 11(a) are sized with respect to the number of times in the sensitivity analysis in which a particular solution was determined to be optimal, and the colors are vary from a robustness-focus (yellow) to cost-focus (red). The first y-axis in Fig. 11(b) displays the desalination costs as a percentage relative to the baseline desalination cost and the remaining axes have the same units as in Fig. 9.

The cost-focus solution, with a desalination cost of 490 MNIS and total robustness score of 0.9, is the only favored solution that has a decrease in total desalination production relative to the baseline scenario. While this solution had the lowest total expected cost, the desalination cost only decreased by 3%, indicating that all solutions with less investment in desalination pay more in recourse cost than they save from decreasing desalination investment. On the other end of the spectrum, the robustness focused solution has a desalination cost of 590 MNIS, a 16% increase from the baseline solution, while achieving a robustness score of 0.98. Representing one of the compromises between cost and robustness, the solution with a 5% increase in desalination was the favored solution for 40% of the preference scenarios, the largest of any of the favored solutions. With a w_c range between 0.18 and 0.56, the solution is predominantly selected in robustness-favored ($w_r > 0.5$) scenarios, however, it is the only solution that is selected for both a cost-favored and robustness-favored preference.

4. Discussion

The application of the two-stage framework to the INWSS emphasizes the need for quantity–quality models to manage water supply systems with multi-quality sources under uncertainty. When the Stage

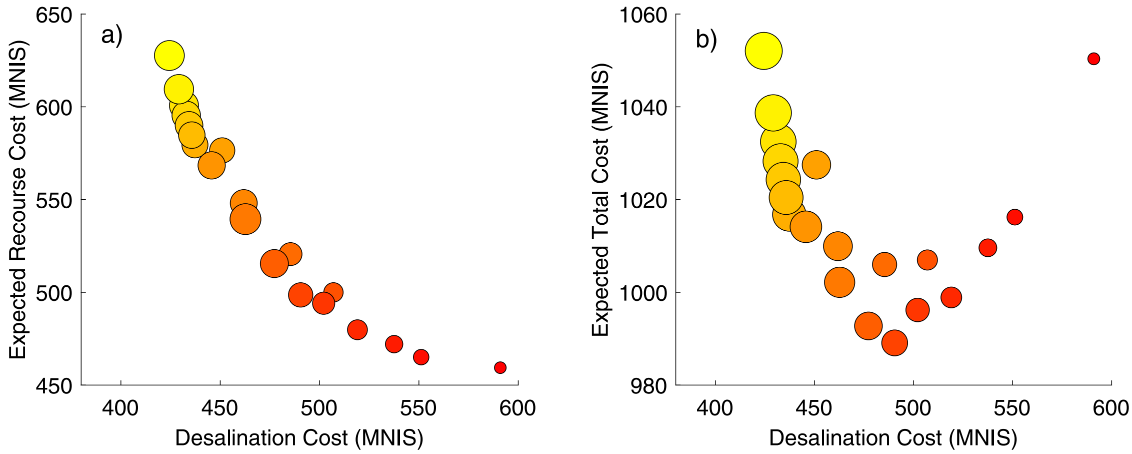

Fig. 10. Two-stage model results. (a) Expected recourse cost versus desalination cost, (b) expected total cost versus desalination cost. The color of each marker corresponds with the associated solution in Fig. 9 and the size of each point corresponds to the variance of the recourse and total cost distributions.

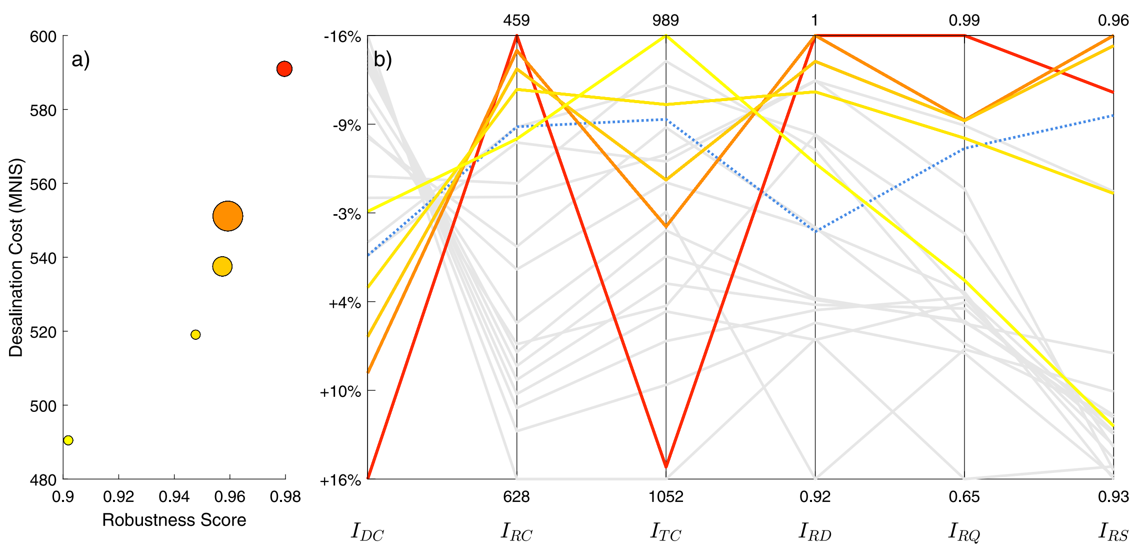

Fig. 11. Optimal solutions ranging from cost-focused to robustness-focused: (a) desalination cost vs. robustness scatter plot of optimal solutions, (b) optimal solutions highlighted on parallel plot.

I model is solved for the baseline hydrological and demand scenarios, the optimal solution utilizes supply from the more saline source, Lake Kinneret, to directly supply the demand zones with high salinity tolerances while mixing with supply from lower salinity sources, desalination plants and aquifers, to remain within stricter salinity bounds for the West Galilee demand zone. As a result of both water outflow via pumping and solute inflow, the salinity level in Lake Kinneret increases throughout the year (Fig. 7(b)), highlighting the need to balance the system objectives of fulfilling system demands, maintaining water quality, and ensuring sustainable water levels in the natural resources. While the optimal solution satisfies all constraints for the baseline scenario, violations with respect to the demand, quality, and sustainability constraints are incurred when the optimal desalination production in the baseline scenario is insufficient under new high stress scenarios. Solutions that register violations represent situations in which hydrological and demand projections underestimate the severity of the actual inflows and consumer demands, resulting in recourse decisions that are unable to compensate for the inadequate supply from the desalination plants. Overall, the demand, water quality, and sustainability violations are all localized in different regions of the scatter plots (see Fig. 8), indicating a diverse set of hydrological and demand input scenarios that will push the system to violate one of the three constraints.

For decision-makers, the complex problem of regional water management under uncertain conditions is compounded by multifaceted goals that can be in conflict with one another. Multicriteria analysis methods are essential to describe inherent tradeoffs in solution alternatives and present the results in an intelligible manner for stakeholders. For the INWSS, a clear economic tradeoff exists between the desalination cost and the expected recourse costs, where greater investments upfront in desalination tend to result in lower expected recourse costs (see Fig. 10(a)). However, greater production from desalination plants only increases the expected total cost up to a point, as increases in desalination investment past a critical point cost more than the savings gained in the expected recourse costs. Furthermore, when managing uncertain outcomes, decision-makers are not only interested in the expected costs, but in the range of potential costs. In this view, an increase in desalination investment results in a decrease in the variance of the recourse and total costs, indicating that paying in advance for greater desalination production decreases the uncertainty of system performance and hedges against extreme outcomes. Another intricacy in the management of regional water systems is the balance between system operational costs and system robustness, a tradeoff that is revealed in the INWSS decision alternatives through adjusting stakeholder weights in the PROMETHEE II method. All solutions that increased the desalination investment resulted in greater robustness (see Fig. 11), where the maximally robust solution increased the desalination investment by 16% from the baseline cost. Likewise, the solution optimized strictly for the least total cost was the only solution that recommends a decrease in upfront desalination investment, albeit only by 3% of the baseline investment.

Aside from the identification of patterns and tradeoffs in the results, multicriteria analysis also serves the benefit of directly implementing stakeholder preferences into the decision-making process. By assessing a wide range of future scenarios and computing the effects of implementing different decisions, the proposed framework allows for stakeholders to assign their preferences a posteriori to determine the decision alternative that most closely aligns with their choices. Implementation of stakeholder preferences a posteriori allows for the rapid evaluation of sets of different preferences and has the advantage of concurrent identification of compromises between stakeholder conflicts and subsequently, minimization of resource expenditures to resolve those conflicts. For example, out of the final decision alternatives, 40% of the cost-robustness preference scenarios converged to the same solution, which also proved to dominate in situations when both cost and robustness were respectively favored. Given the intricate and complex nature of water resource systems, as well as the diverse interests of stakeholders, a participatory modeling approach is emphasized, which requires close collaboration with stakeholders during model development, implementation, and validation. This approach serves to build trust, foster future collaboration, and promote co-learning amongst the other stakeholders including water managers, water consumers, and policymakers (Basco-Carrera et al., 2017). The proposed research exemplifies such collaborative efforts, where the modeling framework was iteratively developed with the IWA, who in turn provided essential data and feedback to validate modeling assumptions and ensure clarity of presentation. Primary points of emphasis for expanding this approach include increasing stakeholder engagement in areas of scenario analysis, prioritizing the presentation of comprehensible results for stakeholders with various levels of familiarity and expertise, and validating the model with historical events to develop trust in model predictions.

There are many avenues for extending the proposed research into other applications. Future work to improve upon this research should focus on extending the model time horizon to multiple years or decades in order to analyze long-term tradeoffs, adding other sources of uncertainty in water resources systems such as population growth and hydrological recharge to aquifers, and examining potential hazard scenarios such as desalination plant failures. For the INWSS, direct extensions include testing the impact of the transboundary water trading system such as the water-for-energy swap signed between Israel and Jordan (Vohra, 2021), supporting future planning decisions including the addition of a new desalination plant to be built in North Israel (Maariv Online, 2022), changes in water use and future water demand (Kramer et al., 2022). Likewise, the proposed two-stage modeling framework is also applicable to other water-stressed regional water supply systems that must manage different water quality sources, uncertainties, asynchronous decision timelines, and complex objectives. Potential applications include a focus on the energy-water nexus surrounding desalination plants, where the framework can be utilized to help optimize desalination production decisions and account for the interplay between water-for-energy and energy-for-water systems (Sood and Smakhtin, 2014; Helerea et al., 2023). The extension of the proposed framework would require the collection of new data, such as operational energy intensity data, water and energy cost data, penalty costs for violating energy and water production commitments, as well as energy and water departments acquiescent to data sharing and co-coordination. In all applications and future work, a participatory modeling approach is paramount to ensuring applicability of solutions to real-world systems, which is the utmost priority in the search for innovative solutions to water scarcity.

5. Conclusions

In this work, a two-stage optimization model combined with multicriteria decision analysis is proposed as a tool for decision makers to analyze tradeoffs between implementable decisions for regional water systems facing uncertainty. The framework is applied to the INWSS where the effects of upfront investment in desalination on the system robustness and expected operational cost are determined. This method is beneficial for systems which do not require parameterizing the uncertainty with distributions for which sufficient data does not exist, or might not accurately represent future conditions. Furthermore, performing the multicriteria assessment a posteriori allows the model to find a compromise between multiple competing objectives while sampling large number of uncertain scenarios without creating an intractably large problem.

More broadly, this work displays the benefits that desalination investment has on securing the regional water supply under extreme conditions. Motivated by an imbalance between water availability and growing demands, the development of the desalination sector in Israel was made possible through multi-decadal water system planning, significant investment of resources into research and development by the Israeli government, and coordination with desalination and technology companies through public–private partnerships. The insights gained from Israel's pathway to water security provides a blueprint for other regions looking to integrate desalination and other cleaner production technologies into their regional water management strategy. Given the growing trend of desalination around the globe combined with the increase of extreme climate conditions that defy historical trends, this methodology can be adapted and implemented to combat the global challenge of water insecurity.

CRediT authorship contribution statement

Greg Hendrickson: Conceptualization, Methodology, Software, Formal analysis, Visualization, Writing – original draft. **Mashor Housh:** Methodology, Data curation, Writing – review & editing. **Lina Sela:** Conceptualization, Methodology, Writing – review & editing, Supervision, Funding acquisition.

Declaration of competing interest

The authors declare that they have no known competing financial interests or personal relationships that could have appeared to influence the work reported in this paper.

Data availability

The data is available in the supplementary material.

Acknowledgments

The authors would like to thank the Israel Water Authority for their guidance and support during this study. This work has not been formally reviewed by IWA. The views expressed in this document are solely those of the authors and do not necessarily reflect those of the agency. IWA does not hold any responsibility over the data and does not endorse any products mentioned in this publication. This work was supported in part by the National Science Foundation under Grant 1943428, 2015658, and 1828974.

Appendix A. Supplementary data

Supplementary material related to this article can be found online at https://doi.org/10.1016/j.jclepro.2023.137785.

References

Abokifa, A.A., Xing, L., Sela, L., 2020. Investigating the impacts of water conservation on water quality in distribution networks using an advection-dispersion transport model. Water 12 (4), 1033. http://dx.doi.org/10.3390/w12041033.

Ahmed, M., Shayya, W.H., Hoey, D., Al-Handaly, J., 2001. Brine disposal from reverse osmosis desalination plants in Oman and the United Arab Emirates. Desalination 133 (2), 135–147. http://dx.doi.org/10.1016/S0011-9164(01)80004-7.

Alidi, A.S., Al-Faraj, T.N., 1994. Goal programming model for distributing and blending desalinized water. J. Water Resour. Plan. Manag. 120 (3), 267–275. http://dx.doi.org/10.1061/(ASCE)0733-9496(1994)120:3(267), Publisher: American Society of Civil Engineers.

Arora, P., Deepali, Varshney, S., 2016. Analysis of k-means and k-medoids algorithm for big data. Procedia Comput. Sci. 78, 507–512. http://dx.doi.org/10.1016/j.procs.2016.02.095.

Avni, N., Eben-Chaim, M., Oron, G., Eben-Chaim, M., Oron, G., 2012. The impact of large scale desalination on water quality: an operational perspective. pp. 2810–2819. http://dx.doi.org/10.1061/41114(371)290, Publisher: American Society of Civil Engineers.

Avni, N., Eben-Chaime, M., Oron, G., 2013. Optimizing desalinated sea water blending with other sources to meet magnesium requirements for potable and irrigation waters. Water Res. 47 (7), 2164–2176. http://dx.doi.org/10.1016/j.watres.2013.01.018.

Basco-Carrera, L., Warren, A., van Beek, E., Jonoski, A., Giardino, A., 2017. Collaborative modelling or participatory modelling? A framework for water resources management. Environ. Model. Softw. 91, 95–110. http://dx.doi.org/10.1016/j.envsoft.2017.01.014.

Ben-Tal, A., Goryashko, A., Guslitzer, E., Nemirovski, A., 2004. Adjustable robust solutions of uncertain linear programs. Math. Program. 99 (2), 351–376. http://dx.doi.org/10.1007/s10107-003-0454-y.

Booker, J.F., Michelsen, A.M., Ward, F.A., 2005. Economic impact of alternative policy responses to prolonged and severe drought in the Rio Grande Basin. Water Resour. Res. 41 (2), http://dx.doi.org/10.1029/2004WR003486.

Borgomeo, E., Mortazavi-Naeini, M., Hall, J.W., Guillod, B.P., 2018. Risk, robustness and water resources planning under uncertainty. Earth's Future 6 (3), 468–487. http://dx.doi.org/10.1002/2017EF000730.

Boyd, S., Boyd, S.P., Vandenberghe, L., 2004. Convex Optimization. Cambridge University Press.

Brans, J.-P., De Smet, Y., 2016. PROMETHEE methods. In: Multiple Criteria Decision Analysis. Springer, pp. 187–219.

Cohen, D., Shamir, U., Sinai, G., 2000. Optimal Operation of multi-quality water supply systems-i: introduction of the Q-C model. Eng. Optim. 32 (5), 549–584. http://dx.doi.org/10.1080/03052150008941313.

Cosgrove, W.J., Loucks, D.P., 2015. Water management: current and future challenges and research directions. Water Resour. Res. 51 (6), 4823–4839. http://dx.doi.org/10.1002/2014WR016869.

Dandy, G., Wu, W., Simpson, A., Leonard, M., 2023. A review of sources of uncertainty in optimization objectives of water distribution systems. Water 15 (1), 136. http://dx.doi.org/10.3390/w15010136, Number: 1 Publisher: Multidisciplinary Digital Publishing Institute.

Darre, N.C., Toor, G.S., 2018. Desalination of water: a review. Curr. Pollut. Rep. 4 (2), 104–111. http://dx.doi.org/10.1007/s40726-018-0085-9.

Dore, M.H., 2005. Climate change and changes in global precipitation patterns: what do we know? Environ. Int. 31 (8), 1167–1181.

Draper, A.J., Jenkins, M.W., Kirby, K.W., Lund, J.R., Howitt, R.E., 2003. Economic-engineering optimization for California water management. J. Water Resour. Plan. Manag. 129 (3), 155–164. http://dx.doi.org/10.1061/(ASCE)0733-9496(2003)129:3(155), Publisher: American Society of Civil Engineers.

Elmusa, S.S., 1995. The Jordan-Israel water agreement: A model or an exception? J. Palest. Stud. 24 (3), 63–73.

Fisher, F.M., Arlosoroff, S., Eckstein, Z., Haddadin, M., Hamati, S.G., Huber-Lee, A., Jarrar, A., Jayyousi, A., Shamir, U., Wesseling, H., 2002. Optimal water management and conflict resolution: The Middle East Water Project. Water Resour. Res. 38 (11), 25–1–25–17. http://dx.doi.org/10.1029/2001WR000943.

Givati, A., Thirel, G., Rosenfeld, D., Paz, D., 2019. Climate change impacts on streamflow at the upper Jordan River based on an ensemble of regional climate models. J. Hydrol.: Reg. Stud. 21, 92–109. http://dx.doi.org/10.1016/j.ejrh.2018.12.004.

Gophen, M., Meron, M., Levin-Orlov, V., Tsipris, Y., Peres, M., 2020. Climate change, regional water balance and land use policy, in the watershed of Lake Kinneret (Israel). Open J. Ecol. 10 (04), 200–224. http://dx.doi.org/10.4236/oje.2020.104014.

Gough, J.D., Ward, J.C., 1996. Environmental decision-making and lake management. J. Environ. Manag. 48 (1), 1–15. http://dx.doi.org/10.1006/jema.1996.0063.

Haimes, Y.Y., 1977. Sensitivity, responsivity, stability and lrreversibility as multiple objectives in civil systems. 1.

Helerea, E., Calin, M.D., Musuroi, C., 2023. Water energy nexus and energy transition—a review. Energies 16 (4), 1879. http://dx.doi.org/10.3390/en16041879.

Herman, J.D., Zeff, H.B., Reed, P.M., Characklis, G.W., 2014. Beyond optimality: multistakeholder robustness tradeoffs for regional water portfolio planning under deep uncertainty. Water Resour. Res. 50 (10), 7692–7713. http://dx.doi.org/10.1002/2014WR015338.

Housh, M., 2011. Optimal Multi-Year Management of Regional Water Resources Systems Under Uncertainty (Ph.D. thesis). Technion - Israel Institute of Technology.

Housh, M., Aharon, T., 2021. Info-gap models for optimal multi-year management of regional water resources systems under uncertainty. Sustainability 13 (6), 3152. http://dx.doi.org/10.3390/su13063152.

Housh, M., Ostfeld, A., Shamir, U., 2012. Seasonal multi-year optimal management of quantities and salinities in regional water supply systems. Environ. Model. Softw. 37, 55–67. http://dx.doi.org/10.1016/j.envsoft.2012.03.001.

Housh, M., Ostfeld, A., Shamir, U., 2013. Limited multi-stage stochastic programming for managing water supply systems. Environ. Model. Softw. 41, 53–64. http://dx.doi.org/10.1016/j.envsoft.2012.11.006.

Israel Water Authority, 2011. Long-term master plan for the national water sector. URL: https://www.gov.il/BlobFolder/policy/masterplan-main/he/masterplan_Water_Sector_Master_Plan.pdf.

Israeli Ministry of Finance, 2022. General background on water desalination. URL: https://www.gov.il/he/departments/general/project-water-desalination-background. Accessed: 2023-02-01.

Jenkins, M.W., Lund, J.R., Howitt, R.E., Draper, A.J., Msangi, S.M., Tanaka, S.K., Ritzema, R.S., Marques, G.F., 2004. Optimization of California's water supply system: results and insights. J. Water Resour. Plan. Manag. 130 (4), 271–280. http://dx.doi.org/10.1061/(ASCE)0733-9496(2004)130:4(271), Publisher: American Society of Civil Engineers.

Jones, E., Qadir, M., van Vliet, M.T., Smakhtin, V., Kang, S.-m., 2019. The state of desalination and brine production: a global outlook. Sci. Total Environ. 657, 1343–1356. http://dx.doi.org/10.1016/j.scitotenv.2018.12.076.

Kang, D., Lansey, K., 2013. Scenario-based robust optimization of regional water and wastewater infrastructure. J. Water Resour. Plan. Manag. 139 (3), 325–338. http://dx.doi.org/10.1061/(ASCE)WR.1943-5452.0000236, Publisher: American Society of Civil Engineers.

Khan, M., Al-Ghouti, M.A., 2021. DPSIR framework and sustainable approaches of brine management from seawater desalination plants in Qatar. J. Clean. Prod. 319, 128485. http://dx.doi.org/10.1016/j.jclepro.2021.128485.

Kramer, I., Tsairi, Y., Roth, M.B., Alon, T., Mau, Y., 2022. Effects of population growth on Israel's demand for desalinated water. Npj Clean Water 5 (67).

Liu, Y., Guo, H., Zhang, Z., Wang, L., Dai, Y., Fan, Y., 2007. An optimization method based on scenario analysis for watershed management under uncertainty. Environ. Manag. 39 (5), 678–690. http://dx.doi.org/10.1007/s00267-006-0029-9.

Loucks, D.P., Van Beek, E., 2017. Water Resource Systems Planning and Management: An Introduction to Methods, Models, and Applications. Springer.

Maariv Online, 2022. IDE and Bank Hapoalim won the tender for the construction of a desalination plant in the Western Galilee. https://www.maariv.co.il/business/economic/israel/Article-958190 Accessed: 2023-05-13.

McMillan, H.K., Westerberg, I.K., Krueger, T., 2018. Hydrological data uncertainty and its implications. WIREs Water 5 (6), e1319. http://dx.doi.org/10.1002/wat2.1319.

Mehrez, A., Percia, C., Oron, G., 1992. Optimal operation of a multisource and multiquality regional water system. Water Resour. Res. 28 (5), 1199–1206. http://dx.doi.org/10.1029/91WR02693.

Mekorot, Israeli National Water Company, 2022. Water resource management. URL: https://www.mekorot-int.com/water-resources/.

Moody, P., Brown, C., 2013. Robustness indicators for evaluation under climate change: Application to the upper Great Lakes. Water Resour. Res. 49 (6), 3576–3588. http://dx.doi.org/10.1002/wrcr.20228.

Morais, D., Almeida, A., 2006. Group decision model to manage water losses. Pesqui. Oper. 26, 567–584.

Morais, D., Almeida, A., 2007. Water supply system decision making using multicriteria analysis. Water SA 32 (2), 229–236. http://dx.doi.org/10.4314/wsa.v32i2.5247.

Ostfeld, A., Shamir, U., 1993. Optimal operation of multiquality networks. I: steady-state conditions. J. Water Resour. Plan. Manag. 119 (6), 645–662. http://dx.doi.org/10.1061/(ASCE)0733-9496(1993)119:6(645), Publisher: American Society of Civil Engineers.

Parry, M.L., Canziani, O., Palutikof, J., Van der Linden, P., Hanson, C., 2007. Climate Change 2007-Impacts, Adaptation and Vulnerability: Working Group II Contribution to the Fourth Assessment Report of the IPCC, Vol. 4. Cambridge University Press.

Perelman, L., Housh, M., Ostfeld, A., 2013. Least-cost design of water distribution systems under demand uncertainty: the robust counterpart approach. J. Hydroinform. 15 (3), 737–750. http://dx.doi.org/10.2166/hydro.2013.138.

Pudenz, S., Bruggemann, R., Voigt, K., Welzl, G., 2002. Multi-criteria evaluation and decision-support instruments for the long-term development of management strategies. Umweltwiss. Schadst. Forsch. 14 (1), 52–57.

Pulido-Velázquez, M., Andreu, J., Sahuquillo, A., 2006. Economic optimization of conjunctive use of surface water and groundwater at the basin scale. J. Water Resour. Plan. Manag. 132 (6), 454–467. http://dx.doi.org/10.1061/(ASCE)0733-9496(2006)132:6(454), Publisher: American Society of Civil Engineers.

Rajabi, M.M., Ataie-Ashtiani, B., Janssen, H., 2015. Efficiency enhancement of optimized Latin hypercube sampling strategies: application to monte carlo uncertainty analysis and meta-modeling. Adv. Water Resour. 76, 127–139. http://dx.doi.org/10.1016/j.advwatres.2014.12.008.

Ray, P.A., Kirshen, P.H., Watkins, D.W., 2012. Staged climate change adaptation planning for water supply in Amman, Jordan. J. Water Resour. Plan. Manag. 138 (5), 403–411. http://dx.doi.org/10.1061/(ASCE)WR.1943-5452.0000172.

Rimmer, A., Givati, A., Samuels, R., Alpert, P., 2011. Using ensemble of climate models to evaluate future water and solutes budgets in Lake Kinneret, Israel. J. Hydrol. 410 (3–4), 248–259. http://dx.doi.org/10.1016/j.jhydrol.2011.09.025.

Sahinidis, N.V., 2017. BARON 21.1.13: Global optimization of mixed-integer nonlinear programs. User's Manual.

Sen, S., Higle, J.L., 1999. An introductory tutorial on stochastic linear programming models. Interfaces 29 (2), 33–61.

Shemer, H., Semiat, R., 2017. Sustainable RO desalination – energy demand and environmental impact. Desalination 424, 10–16. http://dx.doi.org/10.1016/j.desal.2017.09.021.

Slater, Y., Finkelshtain, I., Reznik, A., Kan, I., 2020. Large-scale desalination and the external impact on irrigation-water salinity: Economic analysis for the case of Israel. Water Resour. Res. 56 (9), http://dx.doi.org/10.1029/2019WR025657.

Sood, A., Smakhtin, V., 2014. Can desalination and clean energy combined help to alleviate global water scarcity? JAWRA J. Am. Water Resour. Assoc. 50 (5), 1111–1123. http://dx.doi.org/10.1111/jawr.12174.

Srdjevic, B., Medeiros, Y.D.P., Faria, A.S., 2004. An objective multi-criteria evaluation of water management scenarios. Water Resour. Manag. 18 (1), 35–54. http://dx.doi.org/10.1023/B:WARM.0000015348.88832.52.

Tu, M.-Y., Tsai, F.T.-C., Yeh, W.W.-G., 2005. Optimization of water distribution and water quality by hybrid genetic algorithm. J. Water Resour. Plan. Manag. 131 (6), 431–440. http://dx.doi.org/10.1061/(ASCE)0733-9496(2005)131:6(431), Publisher: American Society of Civil Engineers.

Vahid Pakdel, M.J., Sohrabi, F., Mohammadi-Ivatloo, B., 2020. Multi-objective optimization of energy and water management in networked hubs considering transactive energy. J. Clean. Prod. 266, 121936. http://dx.doi.org/10.1016/j.jclepro.2020.121936.

Vishnupriyan, J., Arumugam, D., Kumar, N.M., Chopra, S.S., Partheeban, P., 2021. Multi-criteria decision analysis for optimal planning of desalination plant feasibility in different urban cities in India. J. Clean. Prod. 315, 128146. http://dx.doi.org/10.1016/j.jclepro.2021.128146.

Vohra, A., 2021. Water-for-energy is better than land-for-peace. URL: https://foreignpolicy.com/2021/12/16/water-for-energy-is-better-than-land-for-peace/. Accessed: 2023-02-01.

Watkins, D.W., Kirby, K.W., Punnett, R.E., 2004. Water for the Everglades: application of the South Florida Systems Analysis Model. J. Water Resour. Plan. Manag. 130 (5), 359–366. http://dx.doi.org/10.1061/(ASCE)0733-9496(2004)130:5(359).

Whateley, S., Steinschneider, S., Brown, C., 2014. A climate change range-based method for estimating robustness for water resources supply. Water Resour. Res. 50 (11), 8944–8961. http://dx.doi.org/10.1002/2014WR015956.